Gas Kinetic Scheme for Continuum and Near-Continuum Hypersonic Flows

Wei Liao* and Li-Shi Luo[†]

Old Dominion University, Norfolk, VA 23529, USA

Kun Xu[‡]

The Hong Kong University of Science & Technology, Clear Water Bay, Kowloon, Hong Kong

We present a unified approach for both continuum and near-continuum flows based on the Boltzmann equation and kinetic theory. We use the gas-kinetic scheme (GKS) developed from the linearized Boltzmann equation for the continuum flows and a modified GKS with a variable relaxation time for the near-continuum flows. The gas-kinetic schemes are validated with simulations of the hypersonic flow past a hollow flare at Mach number 9.91 and the shock structures of Argon gas at Mach 8.0 and 9.0. Our results show that the gas-kinetic schemes can indeed simulate both the continuum and near-continuum flows.

I. Introduction

With severe rarefaction effects and/or within shocks of a few mean free path thickness, modeling and simulation of complex hypersonic flows become very challenging for computational fluid dynamics (CFD). Such problems are genuinely multiscale in nature. Outside shocks, the flow is nearly at thermodynamical equilibrium thus they can be adequately described by the continuum theory—the Navier-Stokes equations, which are the governing equations of hydrodynamics. However, within shocks, the flow is far from the thermodynamical equilibrium and cannot be well described by the continuum theory. In dealing with nonequilibrium flows, one has to solve the Boltzmann equation and one of the most commonly used approach is the direct simulation Monte Carlo (DSMC) method.² The DSMC is a stochastic method which is very effective for free-molecular flows with large Knudsen numbers. However, the DSMC method has several limitations. First, it is subject to numerical fluctuations due to its stochastic nature. Thus DSMC simulations require averaging to obtain flow fields of interest, and for time-dependent flows, DSMC simulations require ensemble averaging, which can be prohibitively expensive in terms of computational time for realistic flows. And second, the DSMC method becomes ineffective in the near-continuum flow region, because its time step must be smaller than the mean free time, which is extremely small in the near-continuum flow region. Therefore, in the near-continuum flow regime where the Knudsen number is small or moderate, the computational time required by the DSMC simulations is several order of magnitude longer than that required by conventional CFD methods. Because of these limitations, it is difficult to couple the DSMC method with conventional CFD methods based on direct discretizations of the Navier-Stokes equations, which are deterministic methods characterized by their spatial-temporal accuracies.

In this work we intend to address the difficulty encountered in coupling between the continuum and near-continuum flows. We present a unified approach for both the continuum and near-continuum flows based on the gas-kinetic scheme (GKS), $^{3-5}$ which is based on the Boltzmann equation and kinetic theory, as opposed to other CFD methods based on the continuum theory. In the gas-kinetic scheme, the fluxes are re-constructed from the single particle distribution function f in phase space, which is the (approximated) solution of the Boltzmann equation. The fluxes so obtained possess the non-equilibrium information beyond the linear constitutive laws, and therefore can capture non-equilibrium effects.

^{*}Research Assistant Professor, Department of Mathematics & Statistics, Old Dominion University. Member of AIAA.

[†]Associate Professor, Department of Mathematics & Statistics, Old Dominion University.

[‡]Professor, Department of Mathematics, The Hong Kong University of Science and Technology. Member of AIAA.

In what follow, we will first show the basic theory behind the gas-kinetic scheme (GKS), and describe the formulation of the GKS. We will use the GKS method to simulate (1) the hypersonic flow around a hollow flare at Mach number 9.91^{1,6} and (2) the shock structure of Argon gas at Mach number 8.0 and 9.0.^{7,8} The former is a continuum flow with shock-boundary layer and shock-shock interactions and the latter is near-continuum flow within a hypersonic shock. Our results show that the gas-kinetic scheme has the capability simulate both continuum and near-continuum flows effectively and efficiently.

II. Numerical Methods

A. Gas Kinetic Scheme for Compressible Flows

In the present study, the gas-kinetic scheme developed by Xu^{3,4} is applied to simulate compressible flows. The scheme is briefly described as follows. We begin with the linearized Boltzmann equation⁹

$$\partial_t f + \boldsymbol{\xi} \cdot \boldsymbol{\nabla} f = \mathcal{L}(f, f), \tag{1}$$

where $f := f(\boldsymbol{x}, \boldsymbol{\xi}, \boldsymbol{\zeta}, t)$ is the single particle distribution function of space \boldsymbol{x} , particle velocity $\boldsymbol{\xi}$, particle internal degree of freedom $\boldsymbol{\zeta}$ of dimension Z, and time t, and \mathcal{L} is the linearized collision operator. For the sake of simplicity and without losing generality, we will use the Bhatnagar-Gross-Krook¹⁰ (BGK) approximation of single relaxation time model for \mathcal{L} :

$$\partial_t f + \boldsymbol{\xi} \cdot \boldsymbol{\nabla} f = -\frac{1}{\tau} \left[f - f^{(0)} \right], \tag{2}$$

where τ is the constant collision time and $f^{(0)}$ is the Maxwellian equilibrium distribution function in D dimensions:

$$f^{(0)} = \rho \left(\beta/2\pi\right)^{(D+Z)/2} e^{-\frac{1}{2}\beta(\mathbf{c}\cdot\mathbf{c}+\boldsymbol{\zeta}\cdot\boldsymbol{\zeta})},\tag{3}$$

where $\boldsymbol{c} := (\boldsymbol{\xi} - \boldsymbol{u})$ is the peculiar velocity, $\beta = (k_{\rm B}T)^{-1}$, and ρ , \boldsymbol{u} and T are flow density, velocity and temperature, respectively. The conserved variables are the conserved moments of the collision operator:

$$\rho = \int f d\mathbf{\Xi} = \int f^{(0)} d\mathbf{\Xi},\tag{4a}$$

$$\rho \mathbf{u} = \int f \boldsymbol{\xi} d\boldsymbol{\Xi} = \int f^{(0)} \boldsymbol{\xi} d\boldsymbol{\Xi},\tag{4b}$$

$$\rho E = \rho \epsilon + \frac{1}{2} \rho \mathbf{u}^2 = \frac{1}{2} \int f(\xi^2 + \zeta^2) d\mathbf{\Xi} = \frac{1}{2} \int f^{(0)}(\xi^2 + \zeta^2) d\mathbf{\Xi}, \tag{4c}$$

where E is the specific total energy and $\epsilon := \frac{1}{2}(D+Z)k_{\rm B}T$ is the specific internal energy, and $\Xi := (\xi, \zeta)$ denotes the single particle velocity space, including the internal degrees of freedom. The Maxwellian equilibrium leads to the equipartition of energy among degrees of freedom, *i.e.*, each degree of freedom shares the same amount of energy $k_{\rm B}T/2$ at equilibrium.

By integrating along the characteristics, one can obtain the following solution of the BGK equation (2):

$$f(\mathbf{x} + \boldsymbol{\xi}t, t) = e^{-t/\tau} f_0 + \frac{1}{\tau} \int_0^t f^{(0)}(\mathbf{x}', \boldsymbol{\xi}, \boldsymbol{\zeta}, t') e^{(t'-t)/\tau} dt',$$
 (5)

where $\mathbf{x}' := \mathbf{x} + \boldsymbol{\xi} t'$, and the initial state $f_0 := f(\mathbf{x}, \boldsymbol{\xi}, \boldsymbol{\zeta}, t = 0)$. The gas-kinetic scheme (GKS) is formulated based on the above equation. With f_0 and $f_0^{(0)} := f^{(0)}(\mathbf{x}, \boldsymbol{\xi}, \boldsymbol{\zeta}, t = 0)$ given, one can construct approximate solution for f at a later time t > 0.

The gas-kinetic scheme is a finite volume method for compressible flows. Thus, the values of hydrodynamic variables, represented by \mathbf{W} , are given at cell centers, while the values of fluxes, represented by \mathbf{F}_{α} , are needed at cell boundaries. Unlike conventional CFD methods which evaluate fluxes from the hydrodynamics variables, the gas-kinetic scheme computes the numerical fluxes from the distribution function f. We shall limit our discuss in two dimensions (2D), in which the total number of internal degrees of freedom $Z = (5-3\gamma)/(\gamma-1)+1$, which accounts for the random motion in the z-direction and two rotational degrees of freedom.

For the sake of convenience, we shall use the following notation for the vectors of (D+2) dimensions:

$$\Psi := (1, \xi_1, \xi_2, (\xi^2 + \zeta^2)/2)^\mathsf{T},\tag{6a}$$

$$\mathbf{W} := (\rho, \rho u_1, \rho u_2, \rho E)^{\mathsf{T}} = \int f \mathbf{\Psi} d\mathbf{\Xi} = \int f^{(0)} \mathbf{\Psi} d\mathbf{\Xi}, \tag{6b}$$

$$\mathbf{F}_{\alpha} := \int f \mathbf{\Psi} \xi_{\alpha} d\mathbf{\Xi}, \qquad \alpha \in \{x, y\} := \{1, 2\}, \tag{6c}$$

$$\mathbf{h} := (\rho, u_1, u_2, T)^{\mathsf{T}}, \qquad \mathbf{h}' := (\rho^{-1}, \beta u_1, \beta u_2, \frac{1}{2} [\beta(c^2 + \zeta^2) - (D + Z)] T^{-1})^{\mathsf{T}}, \tag{6d}$$

where and T denotes the transpose operator. In the above notations, Ψ , W, \mathbf{F}_{α} and h have the collisional invariants, the conserved quantities, the flux along α -axis and the primitive variables as their components, respectively.

To simplify the ensuing discussion, we will only show the construction of the GKS in one dimension. Bear in mind that the GKS is a genuine multidimensional scheme. Because the advection operator in the Boltzmann equation is linear, operator splitting among D coordinates can be applied. Denote a cell center at x coordinate by x_i , and its left and right cell boundaries by $x_{i-1/2}$ and $x_{i+1/2}$, respectively. For simplicity we set initial time $t_0 = 0$, then the solution (5) at the position x and time t is:

$$f(x,t) = e^{-t/\tau} f_0(x - \xi_1 t) + \frac{1}{\tau} \int_0^t f^{(0)}(x',t') e^{-(t-t')/\tau} dt', \tag{7}$$

where $x' := x - \xi_1(t - t')$ is x coordinate of the particle trajectory. In the above equation we omit the variables in f which remain unchanged in time. Initially, only the values of hydrodynamic variables, ρ , ρu and ρE are given at cell center x_i , but fluxes are to be evaluated at the cell boundaries $x_{i\pm 1/2}$. Therefore, both f_0 and $f^{(0)}(x', t')$ in the above equation are to be constructed from the hydrodynamics variable through the Boltzmann equation and Taylor expansion.

We can formally write the BGK equation (2) as the following:

$$f = f^{(0)} - \tau d_t f, \qquad d_t := \partial_t + \boldsymbol{\xi} \cdot \boldsymbol{\nabla}.$$
 (8)

Thus, f can be solved iteratively, starting with $f = f^{(0)}$ on the right hand side of the above equation. For the purpose of simulating the Navier-Stokes equation, $f = f^{(0)} - \tau d_t f^{(0)}$ is sufficient. Therefore, the initial value can be approximated as

$$f_0 \approx [1 - \tau(\partial_t + \xi_1 \partial_x)] f^{(0)} = f^{(0)} [1 - \tau \mathbf{h}' \cdot (\partial_t + \xi_1 \partial_x) \mathbf{h}]$$
(9)

In addition, the equilibrium can be expanded in its Taylor series about x = 0:

$$f^{(0)}(x,t) \approx [1 + x\partial_x]f^{(0)}(0,t) = f^{(0)}(0,t)[1 + x\mathbf{h}' \cdot \partial_x\mathbf{h}].$$
(10)

By substituting Eq. (10) into Eq. (9) we have:

$$f_0(x,t) \approx f^{(0)}(0,t) \left[1 + x\mathbf{h}' \cdot \partial_x \mathbf{h} \right] \left[1 - \tau \mathbf{h}' \cdot (\partial_t + \xi_1 \partial_x) \mathbf{h} \right] = f^{(0)}(0,t) \left[1 + ax - \tau (a\xi_1 + A) \right], \tag{11}$$

where $a = \mathbf{h}' \cdot \partial_x \mathbf{h}$ and $A = \mathbf{h}' \cdot \partial_t \mathbf{h}$ are functions of $\boldsymbol{\xi}$, and hydrodynamic variables, ρ , \boldsymbol{u} and T and their first order derivatives, and they are related by the compatibility condition for f:

$$\int f^{(n)} \mathbf{\Psi} d\mathbf{\Xi} = \mathbf{0}, \qquad \forall \, n > 0.$$

Therefore, the compatibility condition

$$\int f^{(1)} d\mathbf{\Xi} = -\tau \int d_t f^{(0)} d\mathbf{\Xi} = -\tau \int (A + a\xi_1) f^{(0)} d\mathbf{\Xi} = 0$$

leads to the relation between A and a:

$$\int Af^{(0)}d\Xi = -\int af^{(0)}\xi_1 d\Xi.$$
 (12)

As for $f^{(0)}(x, t)$ in the integrand of Eq. (7), it can be evaluated by its Taylor expansion:

$$f^{(0)}(x,t) \approx (1+t\partial_t + x\partial_x)f^{(0)}(0,0) = f^{(0)}(0,0)[1+\mathbf{h}'\cdot(t\partial_t + x\partial_x)\mathbf{h}] = f^{(0)}(0,0)(1+\bar{A}t+\bar{a}x), \quad (13)$$

where \bar{a} and \bar{A} are similar to a and A, respectively.

Assuming the hydrodynamic variables are discontinuous at the cell boundaries (or interfaces) of $x_{i+1/2} = 0$, then the values of the equilibrium $f^{(0)}$ in both side of the cell boundary have to be evaluated differently. The value on the left side, the hydrodynamic variables \mathbf{h} are interpolated to the cell boundary $x_{i+1/2}^-$ from left with two points left and one point right of $x_{i+1/2}$, and the left equilibrium value $f_{\rm L}^{(0)}$ is computed from the hydrodynamic variables at $x_{i+1/2}^-$. Similarly, the right equilibrium value $f_{\rm R}^{(0)}$ are evaluated from the hydrodynamic variables interpolated to the $x_{i+1/2}^+$ from right with two points right and one point left of $x_{i+1/2}$. Consequently, we have

$$f_0(x,t) = [1 + a_{\rm R}(x - \tau \xi_1) - \tau A_{\rm R}]H(x)f_{\rm R}^{(0)}(0,t) + [1 + a_{\rm L}(x - \tau \xi_1) - \tau A_{\rm L}]H(-x)f_{\rm L}^{(0)}(0,t),$$
(14a)
$$f^{(0)}(x,t) = [1 + H(-x)\bar{a}_{\rm L}x + H(x)\bar{a}_{\rm R}x + \bar{A}t]f^{(0)}(0,0),$$
(14b)

where H(x) is the Heaviside function. Finally, the value of f at a cell boundary can be obtained by substituting the above equations of $f_0(x, t)$ and $f^{(0)}(x, t)$ into Eq. (7):

$$f(x_{i+1/2}, t) = \left\{ \left[(1 - \bar{A}\tau)(1 - e^{-t/\tau}) + \bar{A}t \right] + \left[(t + \tau)e^{-t/\tau} - \tau \right] \left[\bar{a}_{L}H(\xi_{1}) + \bar{a}_{R}H(-\xi_{1}) \right] \xi_{1} \right\} f_{0}^{(0)} + e^{-t/\tau} \left\{ \left[(1 - \xi_{1}(t + \tau)a_{L}) - \tau A_{L} \right] H(\xi_{1}) f_{0L}^{(0)} + \left[(1 - \xi_{1}(t + \tau)a_{R}) - \tau A_{R} \right] H(-\xi_{1}) f_{0R}^{(0)} \right\}, \quad (15)$$

where $f_0^{(0)}$, $f_{0L}^{(0)}$ and $f_{0R}^{(0)}$ are initial values of $f^{(0)}$, $f_{L}^{(0)}$ and $f_{R}^{(0)}$ evaluated at cell boundary $x_{i+1/2}$. With f given at cell boundaries, the time-dependent fluxes can be evaluated:

$$\mathbf{F}_{\alpha}^{i+1/2,j} = \int \xi_{\alpha} \mathbf{\Psi} f(x_{i+1/2}, t) d\mathbf{\Xi}$$
 (16)

By integrating the above equation over each time step, we obtain the total fluxes:

$$\bar{\mathbf{F}}_{x}^{i\pm 1/2,j} = \int_{0}^{\Delta t} \mathbf{F}_{x}^{i\pm 1/2,j} dt, \qquad \bar{\mathbf{F}}_{y}^{i,j\pm 1/2} = \int_{0}^{\Delta t} \mathbf{F}_{y}^{i,j\pm 1/2} dt. \tag{17}$$

Then the finite volume formulation for the flow governing equations can be written as:

$$\mathbf{W}_{ij}^{n+1} = \mathbf{W}_{ij}^{n} - \frac{1}{\Lambda x} (\bar{\mathbf{F}}_{x}^{i+1/2,j} - \bar{\mathbf{F}}_{x}^{i-1/2,j}) - \frac{1}{\Lambda y} (\bar{\mathbf{F}}_{y}^{i,j+1/2} - \bar{\mathbf{F}}_{y}^{i,j-1/2}), \tag{18}$$

which is used to update the flow field.

B. Modified Gas Kinetic Scheme for Near Continuum Flows

In the gas-kinetic scheme for compressible flows, the particle collision time is only related with the local macroscopic flow variables through

$$\tau = \mu/p$$

where μ is the dynamic viscosity and p is the pressure. The relaxation time τ is a constant for the isothermal continuum flows. In the near-continuum or transition flow regime, τ is no longer a function of hydrodynamic variables alone. For example, within a hypersonic shock, the particle collision time would depend on the hydrodynamic variables as well as their derivatives. In other words, the simple constitutive relations in the framework of continuum theory are no longer valid in the non-equilibrium flows. To accurately compute shock structures, for which the Navier-Stokes equation is no longer valid, one would need to solve the Boltzmann equation, by using Direct Simulation Monte Carlo (DSMC) method, for instance. In the present work we shall use a modified GKS^{11,12} for such a purpose.

The basic idea behind the modified GKS for shock structures is the following. We know that the conservation laws are valid everywhere, even within shock. What breaks down within shocks are the linear

constitutive relations. The shock structures are of the order of the mean free path. Within shocks the mean free time τ would not be a constant and it strongly depends on local flow fields and their gradients. We hope that a self-consistent solution of the Boltzmann equation would provide an approximation of τ . In what follows we shall consider a one-dimensional shock structure.

We will use the BGK equation to illustrate our idea:

$$f = f^{(0)} - \tau d_t f = f^{(0)} - \tau (\partial_t + \xi_1 \partial_x) f. \tag{19}$$

Suppose we can modify the relaxation time such that it depends on flow fields and their gradients, and the form of the Navier-Stokes equations remains intact, *i.e.*,

$$f \approx f^{(0)} - \tau^* d_t f^{(0)} := f^{[1]},$$
 (20)

where τ^* is the modified relaxation time. One the other hand, one can iterate Eq. (19) once more:

$$f \approx f^{(0)} - \tau d_t f^{(1)} = f^{(0)} - \tau d_t f^{(0)} + \tau \tau^* d_t^2 f^{(0)} := f^{[2]}, \tag{21}$$

and assume that the modeling of τ^* is sufficiently accurate to take into account of the effects due to higher order derivatives of hydrodynamic variables. Therefore, we have $f^{[1]} \approx f^{[2]}$, which leads to

$$\tau^* d_t f^{(0)} \approx \tau (d_t f^{(0)} - \tau^* d_t^2 f^{(0)}). \tag{22}$$

Then we can obtained the modified relaxation time,

$$\tau^* = \frac{\tau}{1 + \tau(d_t^2 f^{(0)}/d_t f^{(0)})}.$$

The above equation depends on the particle velocity $\boldsymbol{\xi}$ and therefore must be averaged over $\boldsymbol{\xi}$. We consider an average over $\phi(\boldsymbol{\xi})$ to obtain

$$\tau^* = \frac{\tau}{1 + \tau \left\langle d_t^2 f^{(0)} \right\rangle / \left\langle d_t f^{(0)} \right\rangle},\tag{23a}$$

$$\left\langle d_t f^{(0)} \right\rangle := \int d_t f^{(0)} \phi(\boldsymbol{\xi}) f d\boldsymbol{\Xi}, \qquad \left\langle d_t^2 f^{(0)} \right\rangle := \int d_t^2 f^{(0)} \phi(\boldsymbol{\xi}) f d\boldsymbol{\Xi}. \tag{23b}$$

Because the stress and the heat conduction terms are different moments of the distribution function f, the values of τ^* for these terms should also be treated differently. We use $\phi(\xi) = c^2$ for the relaxation time corresponding to the viscosity coefficient and $\phi(\xi) = c_{\alpha}(c^2 + \zeta^2)$ for relaxation time corresponding to the heat conductivity coefficient in α -direction. In effect, $\langle d_t^2 f^{(0)} \rangle$ and $\langle d_t f^{(0)} \rangle$ are computed as the functions of hydrodynamic variables as well as their spatial and temporal derivatives up to second order. An *empirical* nonlinear dynamic limiter is imposed on τ^* :

$$\tau^* = \frac{\tau}{1 + \max[-1/2, \tau \min(\langle d_t^2 f^{(0)} \rangle / \langle d_t f^{(0)} \rangle, 0)]}$$

$$\tag{24}$$

to guarantee that $\tau^* \geq \tau$ and to minimize the large numerical fluctuation caused by vanishingly small $\langle d_t f^{(0)} \rangle$, which can occur in regions outside the shock.

C. Prandtl Number Correction

The relaxation time τ in the BGK model determines both the dynamic viscosity μ and the heat conductivity κ , which results in the unit Prandtl number $\Pr = \mu/\kappa = 1$. However, this defect can be easily removed by simply replacing the constant coefficient τ in the heat flux q by the appropriate one determined by the Prandtl number \Pr in the total energy flux K:^{4,13}

$$\boldsymbol{K}^{\text{new}} = \boldsymbol{K} + \left(\frac{1}{\text{Pr}} - 1\right) \boldsymbol{q}, \qquad \boldsymbol{K} := \frac{1}{2} \int \left(\xi^2 + \zeta^2\right) \boldsymbol{\xi} f \, d\boldsymbol{\Xi}, \tag{25}$$

where q is the time-dependent heat flux:

$$q := \frac{1}{2} \int (c^2 + \zeta^2) c f d\Xi. \tag{26}$$

Since the distribution function f is assumed to be smooth, it can be approximated by

$$f = f_0^{(0)} [1 - \tau(\bar{a}\xi_1 + \bar{A}) + t\bar{A}]. \tag{27}$$

Consequently the heat flux q can be approximated by:

$$q_{\alpha} \approx -\tau \int f_0^{(0)}(\bar{a}\xi_{\alpha} + \bar{A})(\psi_4 - \mathbf{u}_0 \cdot \mathbf{\xi})\xi_{\alpha}d\mathbf{\Xi} := \tau q_{\alpha}', \qquad \psi_4 := \frac{1}{2}(\xi^2 + \zeta^2), \quad \alpha \in \{x, y\} := \{1, 2\}, \quad (28)$$

where $u_0 := (u_0, v_0)$ is the flow velocity at the cell interface and at time t = 0. In the above evaluation of q_{α} , the term $t\bar{A}$ in Eq. (27) has been neglected. This approximation would only affect the temporal accuracy of the GKS. Since all moments needed in Eq. (28) have been computed in the evaluation of the total energy flux K, thus additional effort required to compute K^{new} is negligible. Finally, Eq. (25) can be written as

$$\mathbf{K}^{\text{new}} = \mathbf{K} + \left(\frac{1}{\text{Pr}} - 1\right) \tau \mathbf{q}'. \tag{29}$$

For the near-continuum flows, a modified variable relaxation time τ^* given by Eq. (24) must be used. Because different relaxation times must be used for the viscous stress and the heat flux, as indicated in the discussion following Eqs. (23), Eq. (29) is modified as the following:

$$\mathbf{K}^{\text{new}} = \mathbf{K} + \left(\frac{\tau_{\kappa}^*}{\text{Pr}} - \tau_{\mu}^*\right) \mathbf{q}',\tag{30}$$

where τ_{κ}^* and τ_{μ}^* are the modified relaxation times corresponding to the heat conductivity κ and the viscosity μ , respectively, and they are computed according to Eqs. (23).

III. Results and Discussions

We developed a GKS code based on kinetic theory which can simulate both continuum and near-continuum compressible flows. To validate our code, we simulate two test cases. The first is a hypersonic flow around an axisymmetrical hollow flare with Mach number $Ma = 9.91^{1.6}$ and the second is the shock structure of Argon gas with Ma = 8.0 and $9.0.^{7.8}$ The former is a continuum flow with shock-boundary layer and shock-shock interactions and the latter is the near-continuum flows within hypersonic shocks.

A. Hypersonic Flow around a Hollow Flare

The hypersonic flow around an axisymmetrical hollow flare is a well known testing case for shock-boundary layer and shock-shock interactions¹ and has been used to test various numerical methods. Although the Knudsen number Kn is relatively small (Kn ≈ 0.005) in this case, the existing studies¹⁴ show that the thermodynamic non-equilibrium (rarefaction) gas effects are severe. Complex flow physics in this flow makes it a challenging case for a viscous flow solver to accurately capture the wave interaction.

The free-stream parameters are: Ma = 9.91, p_{∞} = 6.3 (Pa), T_{∞} = 51 (°K) and $T_{\rm w}$ = 293 (°K). These conditions ensure the flow to be laminar flow in the entire domain. In the present work, the computation is carried out on a 241 × 161 mesh which is highly stretched in the radial (y) direction, as illustrated in figure 1(a). The normalized temperature T/T_{∞} and the normalized pressure p/p_{∞} contours obtained by the GKS code are presented in Figs. 1(b) and 1(c), respectively. Complex shock interaction can be observed in the flow field: An attached shock wave is formed at the leading edge. In the meantime, the flow separates upstream of the flare and reattaches at a point on the conical section, which induces a separation shock wave and an attachment shock wave. These three shock waves interact with each other above the end of the flare. The positions of the separation point and attachment point obtained by the GKS in the present study and the existing data obtained by other methods⁶ are presented in Table 1. Clearly the GKS results are in good agreement with existing data.

In figure 2, we compare the pressure coefficient C_p , the skin-friction coefficient C_f and the Stanton number St obtained from the GKS method with the existing data from the DSMC and other methods:⁶

$$C_p := \frac{(p - p_{\infty})}{\frac{1}{2}\rho_{\infty}U_{\infty}^2}, \quad C_f := \frac{\tau_{\mathbf{w}}}{\frac{1}{2}\rho_{\infty}U_{\infty}^2}, \quad \text{St} := \frac{\kappa(\partial_{\mathbf{n}}T)_{\mathbf{w}}}{\rho_{\infty}u_{\infty}(H_0 - H_{\mathbf{w}})},$$

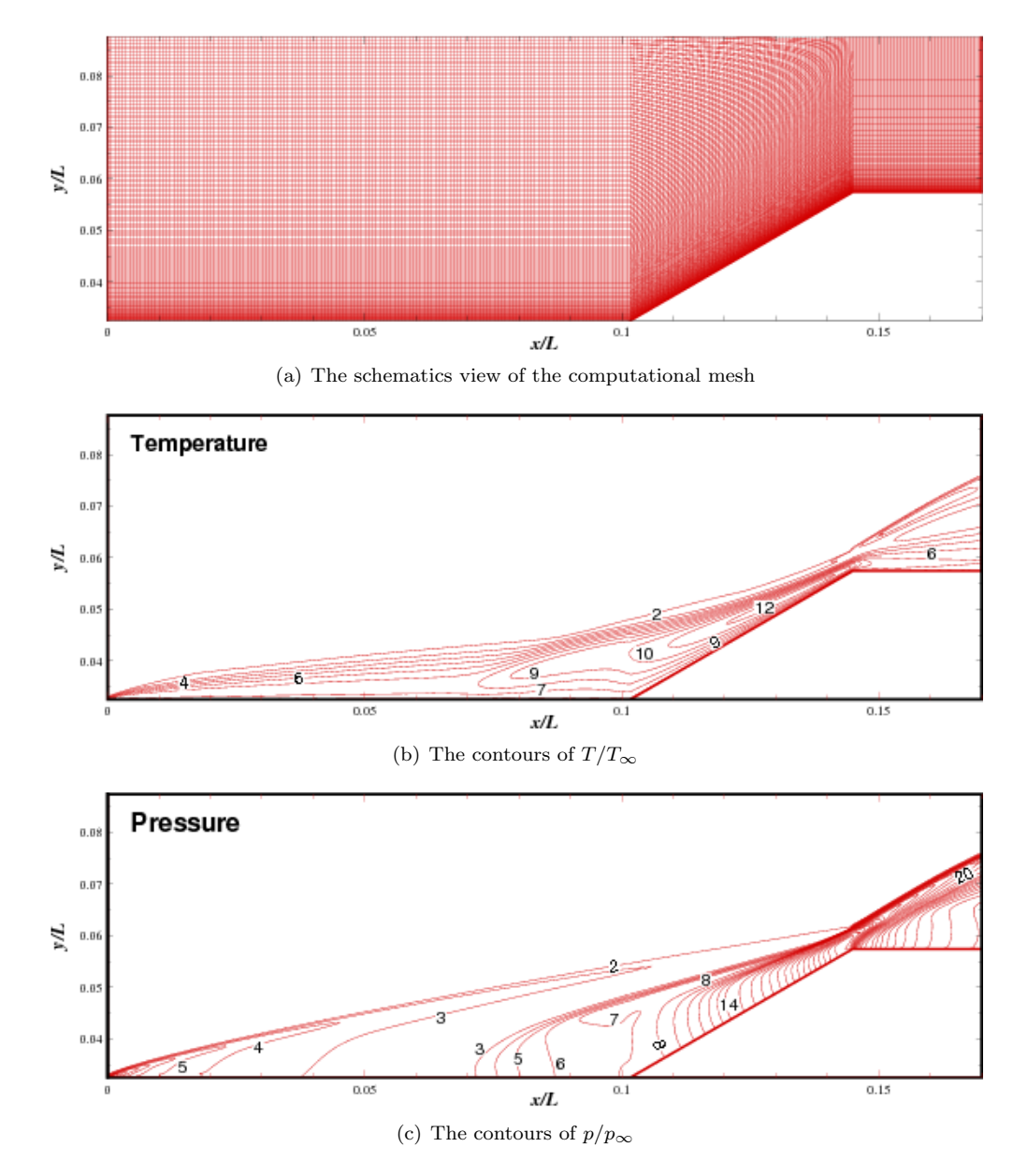


Figure 1. Hypersonic flow around a hollow flare with Ma = 9.91.

Table 1. Separation and reattachment lengths for the flow past a hollow flare. The GKS results of the present study vs. the existing data.⁶

Abscissa x/L	NS	DSMC	GKS	Exp.
Separation	0.74 – 0.75	0.76	0.745	0.76 ± 0.01
Reattachment	1.33	1.32	1.341	1.34 ± 0.01

where H is the enthalpy, κ is the thermal conductivity, $\tau_{\rm w}$ is the wall shear stress, and n denotes the normal direction of the wall. To amplify the differences, we use logarithm scale in y-axis for these figures. For C_f and St, the GKS results are in excellent agreement with the existing data.^{6,14} For the wall pressure distribution C_p , we observe a small discrepancy between the GKS result and the experimental data⁶ near the entrance. This still remains as an open issue⁶ subject to future investigation and it may be due to the uncertainty of inflow conditions.¹⁵

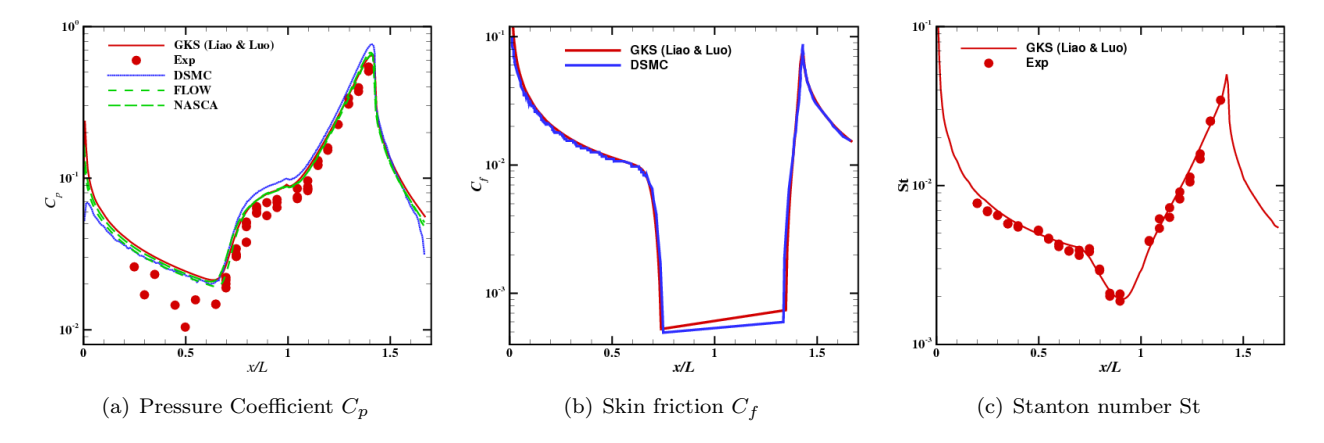


Figure 2. The hypersonic flow around a hollow flare with Ma = 9.91.

Figure 3 shows density profiles at two different cross-sections x/L = 0.6 and 0.76. The inverse phenomena appears within the region 0.6 < x/L < 0.76. Again, the GKS results agree well with existing experimental data.⁶ It is worthy noting that the GKS results accurately predict the radial shock position.

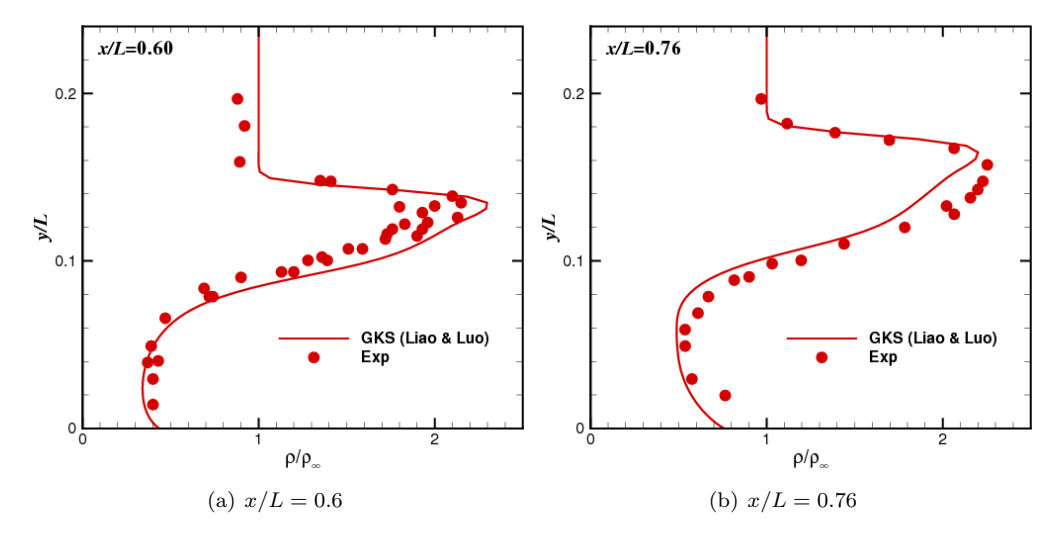


Figure 3. Density profiles at different positions in the hypersonic flow around a hollow flare with Ma = 9.91.

B. Non-Equilibrium Shock Structures in Argon Gas with Ma = 8.0 and 9.0

High Mach number shock waves represent flow conditions far from the thermodynamic equilibrium. In this work, a stationary shock wave in atomic Argon gas with Mach numbers Ma = 8.0 and 9.0 is used to validate the modified GKS method for calculations of the shock structure under hypersonic conditions.

The computational domain is covered with an uniform grid with no less than 30 grid points inside the shock. The entire domain is sufficiently large so the shock does not disturb both the upstream and downstream. The upstream flow conditions are: the Mach number Ma = 8.0 or 9.0, and the temperature $T_1 = 300$ (°K). The downstream flow conditions can be determined by the Rankine-Hugoniot relations. Other parameters are: $\gamma = 5/3$, Pr = 2/3 and $\mu \propto T^s$, where $s = 1/2 + 2/(\nu - 1)$ and ν is the power of the intermolecular force law.² For the case of Ma = 8.0, $\nu = 12$ and the upstream mean free path λ_1 is defined by:²

$$\lambda_1 = \frac{2\mu(7 - 2s)(5 - 2s)}{15\rho_1\sqrt{2\pi RT_1}}. (31)$$

And for the case of Ma = 9.0, $\nu = 7.5$ and λ_1 is defined by:⁸

$$\lambda_1 = \frac{16\mu}{5\rho_1\sqrt{2\pi RT_1}}. (32)$$

These two different definitions of λ_1 are used so the comparisons with existing data^{7,8} can be made.

Figure 4 shows the density and temperature profiles for Argon gas computed by the gas-kinetic schemes with and without the modification of the collision time τ , together with the DSMC results by Bird⁷ and experimental data by Alsmeyer.⁸ The distance x is normalized by the upstream mean free path λ_1 . The density and temperature distribution are defined as, respectively

$$\frac{\delta\rho}{\Delta\rho} := \frac{(\rho - \rho_1)}{(\rho_2 - \rho_1)}, \qquad \frac{\delta T}{\Delta T} := \frac{(T - T_1)}{(T_2 - T_1)},$$

where ρ_2 and T_2 are the downstream density and temperature, respectively. Figure 4 shows that at Ma = 8.0 and 9.0, the present results agree very well with the DSMC results and experimental data. For Mach 8.0 case, the shock thickness and separation distance between the density ρ and the temperature T predicted by the modified GKS method agree very well with those predicted by DSMC.⁷ In contrast, the GKS method with a constant τ , which is effectively a Navier-Stokes solver, under-predicts the shock width and the distance between ρ and T.

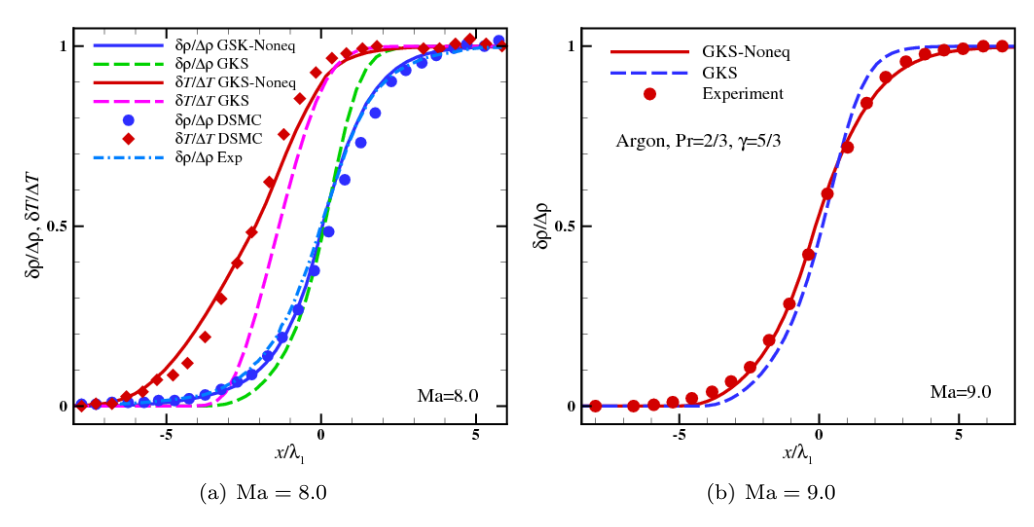


Figure 4. The density and temperature profiles of Argon gas inside the shock layer at Ma = 8.0 and 9.0.

Figure 5 shows the distributions of normal heat flux q_x and the stress τ_{xx} from the GKS and the modified GKS methods compared with the DSMC results.⁷ The normal heat flux q_x and the stress τ_{xx} are defined by

$$q_x := \frac{\kappa \partial_x T}{\rho_1 (2RT_1)^{3/2}}, \qquad \tau_{xx} := \frac{4}{3} \frac{\mu \partial_x u}{(2\rho_1 RT_1)}.$$

Figure 5 clearly shows that the modified GKS method with variable relaxation times significantly improves the prediction for the heat flux q_x : Both the magnitude and the width of the distribution of q_x are accurately obtained by the modified GKS method and the GKS results agree very well with the DSMC data.⁷ Although significant improvements have also been made in the calculations for the stress τ_{xx} —the width of τ_{xx} is accurately computed, the modified GKS method still over-predicts the magnitude of τ_{xx} by about 40%. This may be due to the fact that the stress is related to the higher order effects while the current τ^* only takes into account of up to the second order ones. The sources of this discrepancy are the subject of our future studies.

Our results demonstrate that the modified gas-kinetic scheme with variable mean free time τ^* can effectively and accurately compute the shock structure, which is within the extend of a few mean free paths and cannot be accurately computed by conventional CFD methods based on the solutions of the Navier-Stokes equations, as clearly shown in figures 4 and 5.

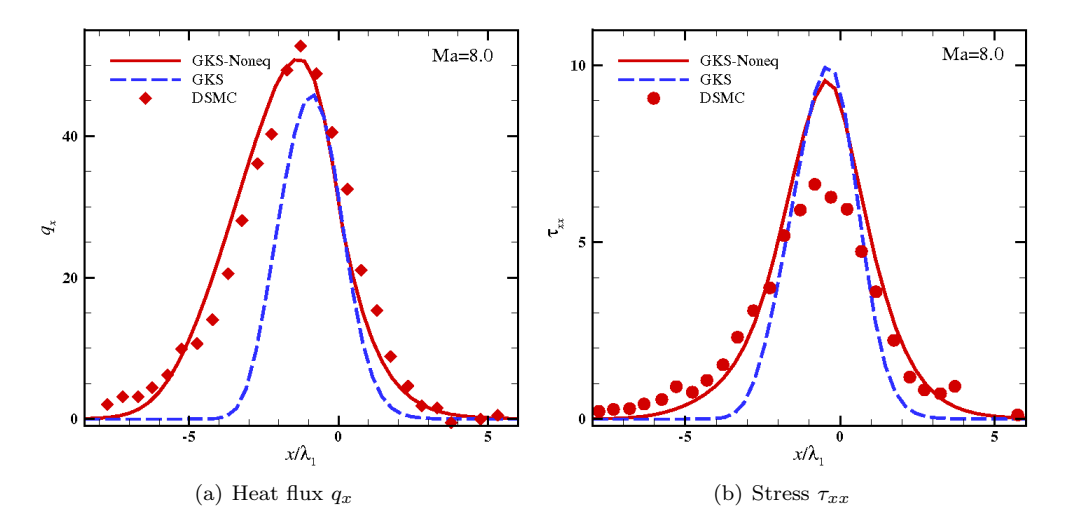


Figure 5. The heat flux and stress inside the shock layer of a Mach-8 shock in Argon gas.

IV. Conclusion

We have demonstrated in this paper the capability of the gas-kinetic schemes for accurately capturing shock-boundary layer interaction and shock structures. In effect, we present a unified approach for continuum and near-continuum hypersonic flows based on the Boltzmann equation and kinetic theory. The numerical results for the hypersonic flow around a hollow flare with Ma=9.91 and the shock structure of Argon gas with Ma=8.0 and 9.0 agree very well with the existing experimental data and other numerical results. We note that conventional CFD methods based on direct discretizations of the Navier-Stokes equations cannot accurately predict shock structures. For non-equilibrium flows such as hypersonic shocks, the advantages of the GKS method over the conventional Navier-Stokes solvers are clearly shown here. Moreover, it takes only under about a minute of CPU time for the shock structure calculation by using the modified GKS method, much faster than the DSMC simulations.

As we indicate in the Introduction, our motivation to formulate a unified approach for continuum and near-continuum flows is to circumvent the difficulties encountered in the coupling between the deterministic CFD and the stochastic DSMC methods for non-equilibrium flows. Our preliminary results presented in this work demonstrate the potential of the kinetic methods, such as the GKS methods, to bridge between conventional CFD methods and other methods for non-equilibrium flows based on the Boltzmann equation. Because the modified GKS method is essentially the GKS method for the compressible Navier-Stokes equations with variable relaxation times depending on the flow variables and their derivatives, which are readily available in the GKS method. Therefore, the GKS methods with and without the variable relaxation times can be run as one code with a switch to turn on or off automatically depending on the local flow information. The modified GKS method can be used to couple a deterministic Boltzmann solver for the solution of the distribution function f sufficiently accurate for particular flows. In this way we hope to simulate non-equilibrium flows with a wide range of the Knudsen number and the Mach number, and this is the subject of our future investigation.

Acknowledgments

The authors are grateful to Dr. Jim N. Moss of NASA Langley Research Center and Drs. Bruno Chanetz and Richard Benay of ONERA for providing the data for the flow past a hollow flare. W. Liao and L.-S. Luo would like to acknowledge the support from the US Department of Defence under AFOSR-MURI project "Hypersonic Transition and Turbulence with Non-equilibrium Thermochemistry" (Dr. J. Schmisseur, Program Manager) and from NASA Langley Research Center under a C&I grant through the NIA Cooperative Agreement Grant NCC-1-02043. K. Xu would like to acknowledge the support from Research Grants Council of the Hong Kong Special Administrative Region, China, under the Project HKUST6102/04E.

References

- ¹Holden, M., "Experimental studies of laminar separated flows induced by shock wave/boundary layer and shock/shock interaction in hypersonic flows for CFD validation," Tech. Rep. AIAA 2000-0930, AIAA, 2000.
 - ²Bird, G. A., Molecular Gas Dynamics and the Direct Simulations of Gas Flows, Oxford Science, Oxford, UK, 1994.
- ³Xu, K., "Gas-kinetic schemes for unsteady compressible flow simulations," The 29th Computational Fluid Dynamics, VKI Lecture Series, Vol. 1998-03, The von Karman Institute for Fluid Dynamics, Rhode-St-Genèse, Belgium, 1998.
- ⁴Xu, K., "A gas-kinetic BGK scheme for the Navier-Stokes equations and its connection with artificial dissipation and Godunov method," *J. Computat. Phys.*, Vol. 171, No. 1, 2001, pp. 289–335.
- ⁵Ohwada, T. and Xu, K., "The kinetic scheme for the full-Burnett equations," *J. Computat. Phys.*, Vol. 201, 2004, pp. 315–332.
- ⁶Gorchakova, N., Kuznetsov, L., Yarygin, V., Chanetz, B., Pot, T., Bur, R., Taran, J. P., Pignche, D., Schulte, D., and Moss, J., "Progress in hypersonic studies using electronic-beam-excited x-ray detection," AIAA J., Vol. 40, No. 4, 2002, pp. 593–598.
 - ⁷Bird, G. A., "Aspects of the structure of strong shock waves," *Phys. Fluids*, Vol. 13, 1970, pp. 1172–1177.
- ⁸Alsmeyer, H., "Density profiles in argon and nitrogen shock waves measured by the absorption of an electron bean," *J. Fluid Mech.*, Vol. 74, 1976, pp. 497–513.
 - ⁹Harris, S., An Introduction to the Theory of the Boltzmann Equation, Dover, Mineola, NY, 2004.
 - ¹⁰Bhatnagar, P., Gross, E., and Krook, M., "A model for collision processes in gases," Phys. Rev., Vol. 94, 1954, pp. 511–525.
- 11 Xu, K. and Tang, L., "Nonequilibrium Bhatnagar-Gross-Krook model for nitrogen shock structure," *Phys. Fluids*, Vol. 16, No. 10, 2004, pp. 3824–3827.
- ¹²Xu, K. and Josyula, E., "Continuum formulation for non-equilibrium shock structure calculation," Comm. Comp. Phys., Vol. 1, No. 3, 2006, pp. 425–450.
- ¹³Woods, L. C., An Introduction to the Kinetic Theory of Gases and Magnetoplasmas, Oxford University Press, Oxford, UK, 1993.
- ¹⁴Li, Q. B., Fu, S., and Xu, K., "Application of gas-kinetic scheme with kinetic boundary conditions in hypersonic flow," AIAA J., Vol. 43, No. 10, 2005, pp. 2170–2176.
- ¹⁵Druguet, M.-C., Candler, G. V., and Nompelis, I., "Effects of numerics on Navier-Stokes computations of hypersonic double-cone flows," AIAA J., Vol. 43, No. 3, 2005, pp. 616–623.